Research Square

Preprints are preliminary reports that have not undergone peer review.
They should not be considered conclusive, used to inform clinical practice,
or referenced by the media as validated information.

Optimization of ultrasound pre-treatment on the chemical composition and structural and thermal properties of cacauí seed powder

Josiana Moreira Mar

josimoreira@ufam.edu.br

Federal University of Amazonas

Daniel de Queiroz Rocha

Federal University of Amazonas

Adriano de Souza Carolino

Federal University of Amazonas

Camila Macena Ruzo

Federal University of Amazonas

Daniel Nascimento Motta

Federal University of Amazonas

Florência João Macamo

Federal University of Amazonas

Erickson Oliveira dos Santos

Samsung Eletrônica da Amazônia

Francisca das Chagas do Amaral Souza

National Institute of Amazonian Research

Valdely Ferreira Kinupp

Federal Institute of Education, Science and Technology of Amazonas

Renilto Frota Correa

Federal Institute of Education, Science and Technology of Amazonas

Edgar Aparecido Sanches

Federal University of Amazonas

Pedro Henrique Campelo

Universidade Federal de Viçosa

Jaqueline de Araújo Bezerra

National Institute of Amazonian Research

Research Article

Keywords: Theobroma speciosum Willd. ex Spreng, ultrasound pre-treatment, bioactive compounds and antioxidant activity

Posted Date: May 25th, 2026

DOI: https://doi.org/10.21203/rs.3.rs-9406280/v1

License: This work is licensed under a Creative Commons Attribution 4.0 International License.
Read Full License

Additional Declarations: No competing interests reported.

Abstract

The study evaluated the effect of ultrasound pre-treatment on the physicochemical, structural, and functional properties of *Theobroma speciosum* Willd. ex Spreng (cacauí) seed powder, focusing on the release of bioactive compounds. The proximate composition indicated low moisture content (2.31–3.98%) and high levels of lipids (25.94–28.92%) and carbohydrates (50.31–54.37%), as well as moderate amounts of proteins (14.69–16.25%) and ash (1.78–2.85%), demonstrating high nutritional value. FTIR analysis confirmed the presence of functional groups typical of lipids, proteins, and polysaccharides, showing that ultrasound promoted changes in intermolecular interactions without compromising the chemical integrity of the matrix. The identification of theacrine highlighted the potential of cacauí as a source of bioactive alkaloids of nutraceutical interest. SEM micrographs showed increased roughness, porosity, and particle fragmentation with increasing ultrasound amplitude and time, indicating cell wall disruption and greater exposure of intracellular compounds. Thermogravimetric analysis revealed a thermal profile typical of lignocellulosic biomass, with small variations in thermal stability after treatment. Antioxidant assays (DPPH, ABTS, and FRAP) and total phenolic content showed a significant increase in antioxidant activity, especially under the C70/12 condition, indicating that acoustic cavitation favors the release of phenolic compounds. The mineral profile showed predominance of K, P, Mg, and Ca, as well as Fe, Zn, Mn, and Cu, reinforcing the nutritional potential of cacauí as a source of essential minerals and a functional ingredient.

1. Introduction

Species of the genus *Theobroma* have attracted increasing scientific interest due to their high nutritional value and potential as a source of bioactive compounds with functional and technological properties (Mar et al., 2024). Among them, *Theobroma speciosum* Willd. ex Spreng (cacauí) stands out for the presence of bioactive metabolites that contribute to antioxidant, nutraceutical, and pharmacological activities. Phenolic compounds are widely recognized for their ability to neutralize free radicals, acting as important antioxidant agents and helping to prevent oxidative stress associated with various chronic diseases (Mar et al., 2021).

In recent years, the search for processing technologies capable of increasing the extraction and bioavailability of bioactive compounds present in plant matrices has intensified. Among these technologies, ultrasound-assisted extraction stands out as an efficient, rapid, and “green” approach, as it reduces processing time and solvent consumption while preserving thermosensitive compounds. Ultrasound is based on the phenomenon of acoustic cavitation, characterized by the formation, growth, and collapse of microbubbles in the liquid medium, generating microjets and shear forces capable of disrupting cellular structures and increasing mass transfer between the solvent and intracellular metabolites (Yusoff et al., 2022).

The application of ultrasound has been widely reported as an efficient strategy to increase the extraction of phenolic compounds, flavonoids, and other secondary metabolites from plant matrices. The effect of

acoustic cavitation promotes modifications in the microstructure of the material, including increased porosity, reduced particle size, and weakening of the cell wall. These structural changes facilitate solvent diffusion and the release of intracellular compounds, contributing to higher levels of bioactive substances and, consequently, greater antioxidant activity of the obtained extracts (González-Silva et al., 2022).

Despite the technological and nutritional potential of cacauí, there are still gaps in the literature regarding the detailed characterization of the physicochemical, structural, and functional properties of its seeds, especially when subjected to emerging processing technologies. In this context, the present study aimed to evaluate the effect of ultrasound pre-treatment on the chemical composition, antioxidant activity, microstructural characteristics, and thermal stability of cacauí seed powder, contributing to expanding knowledge on the use of this Amazonian species as a promising source of bioactive compounds with potential applications in the food, pharmaceutical, and biotechnological industries.

2. Materials and methods

2.1 Sample preparation

Cacauí seed powder was obtained at km 14 in the municipality of Careiro Castanho, Amazonas, Brazil, under SisGen registration nº A9F3E4F, and subsequently subjected to a roasting process. For the ultrasonic treatment, a sample-to-water ratio of 1:10 (w/v) was used. All systems were prepared by sonication using power amplitudes of 20, 40 and 70%, corresponding to different levels of ultrasonic energy density. Treatment times were 4, 8 and 12 min, and the process was carried out in an ice bath to prevent sample overheating. During ultrasonic homogenization, the systems were treated using a 25 mm diameter probe operating at a frequency of 20 kHz and nominal power of 750 W (VibraCell VCX 750, Sonics, Shawnee, OK, USA). After the ultrasound (US) process, excess water was removed with paper towel, and the samples were subsequently freeze-dried (N. C. Santos et al., 2024).

2.2 Antioxidant capacity assessment

The free radical scavenging capacity of the samples was evaluated using the DPPH• and ABTS•⁺ assays, as well as the ferric reducing antioxidant power (FRAP) method (Mar et al., 2025).

For the DPPH• assay, a 100 μM methanolic DPPH• solution was prepared. Samples were diluted to a concentration of 1 mg/mL, and 100 μL of the sample solution was added to 1900 μL of the DPPH• solution. Trolox (100–2000 μM) was used as the standard for the calibration curve. The reaction mixture was kept protected from light at room temperature for 30 min, and absorbance was measured at 515 nm using a microplate reader (Epoch 2, BioTek, Winooski, VT, USA). All analyses were performed in triplicate.

The ABTS•⁺ radical scavenging activity was determined by measuring the reduction in absorbance of the ABTS•⁺ solution in the presence of antioxidant compounds. The reaction was carried out using a sample-to-radical ratio of 1:10, with a reaction time of 6 min. Absorbance was measured at 750 nm using a

microplate reader. The calibration curve was obtained using Trolox as the standard, and the results were expressed as μM Trolox equivalents per mL.

The ferric reducing antioxidant power (FRAP) assay was used to evaluate the ability of the extracts to reduce Fe^{3+} to Fe^{2+} in the presence of the ferric–tripyridyltriazine complex. After incubation of the sample with the FRAP reagent at 37°C for 30 min, absorbance was measured at 593 nm using a UV spectrophotometer. The standard curve was constructed using $FeSO_4$, and the results were expressed as micromolar equivalents of Fe(II) (μM Fe(II)/mL).

2.3 Determination of total phenolic content of extracts (TPC)

Total phenolic content (TPC) was determined using the Folin–Ciocalteu colorimetric method. Initially, the samples were mixed with the Folin–Ciocalteu reagent and allowed to react for 5 min. Subsequently, a 6% sodium bicarbonate solution was added, and the reaction mixture was incubated at room temperature for 90 min. The absorbance was measured at 750 nm using a microplate reader. The results were expressed as milligrams of gallic acid equivalents per milliliter of sample (mg GAE/mL) (Mar et al., 2023).

2.4 LC–ESI–QTOF-MS Qualitative Analysis

Chromatographic separation was performed using an ultra-high-performance liquid chromatography (UHPLC) system (ACQUITY UPLC®, Waters Corp., Milford, MA, USA) equipped with a binary solvent manager and an autosampler. An ACQUITY UPLC® BEH C18 column (1.7 μm particle size) was employed and maintained at 40°C. The autosampler temperature was set at 15°C, and the injection volume was 10 μL.

The mobile phase consisted of (A) ultrapure water with 0.1% formic acid and (B) methanol containing 0.1% formic acid. The flow rate was set at 0.25 mL min^{-1}. The gradient elution program was as follows: 0–15 min, 2–20% B; 15–20 min, 20–40% B; 20–25 min, 40–80% B; 25–27 min, 80–95% B; held at 95% B until 28 min; followed by re-equilibration to initial conditions (2% B) from 28.5 to 30 min. The total run time was 30 min.

Mass spectrometric detection was carried out using a quadrupole time-of-flight mass spectrometer (QTOF-MS) (Xevo G2-XS QTof, Waters Corp.) equipped with an electrospray ionization (ESI) source operating in positive ion mode (ESI+). The instrument was operated in resolution mode with a mass resolving power of approximately 30,000. Data were acquired over an m/z range of 100–1200 Da in continuum mode.

The ion source parameters were set as follows: capillary voltage, 3.0 kV; sampling cone voltage, 40 V; source temperature, 150°C; desolvation temperature, 500°C; cone gas flow, 50 L h^{-1}; and desolvation gas flow, 800 L h^{-1}. The collision energy was applied using a data-independent acquisition (MSE) approach, with low-energy scans at 6 eV and high-energy ramp from 20 to 35 eV to generate fragment ions.

Leucine enkephalin was used as the lock-mass reference ($[M + H]^+$ = m/z 556.2771), infused at 10 μL min^{-1}, with acquisition every 15 s to ensure mass accuracy during the analysis. The system was calibrated using a sodium formate solution over the mass range of m/z 92–1174 prior to analysis. Data acquisition and processing were performed using MassLynx™ software (version 4.2, Waters Corp.). Peak detection, deconvolution, and spectral interpretation were conducted using centroided data with automated isotope and charge state recognition.

2.5 High-performance liquid chromatography with diode array detector (HPLC-DAD) for quantitative analysis

A reverse-phase HPLC system (Shimadzu Corporation, Kyoto, Japan) was employed for the quantification of theacrine (Bento et al., 2026). The chromatographic system consisted of an autosampler (SIL-20A), solvent delivery pumps (LC-20CE), an online degasser (DGU-20A5), a system controller (CBM-20A), a column oven (CTO-20A), and a diode-array detector (SPD-M20A), all controlled by LCsolution software (version 1.25 SP5).

Chromatographic separation was performed using an CORTECS T3 column (4.6 × 100 mm, 2.7 μm particle size; Waters Corporation, Milford, MA, USA). The flow rate was set at 1.0 mL/min, and the injection volume was 10 μL. The mobile phase consisted of 0.1% (v/v) aqueous formic acid (solvent A) and methanol (solvent B). Both samples and mobile phase were filtered through a 0.22 μm polyvinylidene difluoride (PVDF) membrane filter (47 mm diameter; Millipore, USA) and degassed in an ultrasonic bath prior to analysis. The gradient elution program was as follows: 10–60% B over 15 min, 60–80% B at 20 min, 80–100% B at 28 min, followed by re-equilibration to 10% B at 30 min. The column temperature was maintained at 35°C.

The wavelengths for detections were used for confirmation of chromatography peaks and quantification of their corresponding phenolic compounds achieved by comparing their retention time with those of reference standards and by DAD spectra (200 to 600 nm).

Theacrine standard solutions were prepared in ultrapure water. A stock solution (171.50 mg/L) was prepared from certified reference material and used to obtain working standard solutions by serial dilution, freshly prepared on a daily basis. Calibration was performed at 290 nm over the concentration range of 2.3–45.7 mg/L. The method exhibited excellent linearity, with a coefficient of determination (R^2) of 0.9989 and the regression equation $y = 25036x - 9517.4$. The limit of quantification (LOQ) was determined to be 0.22 mg/L, and the method demonstrated acceptable homoscedasticity across the evaluated concentration range.

2.6 Proximate composition

The proximate composition of cacauí seed powders was determined according to standardized analytical procedures. Moisture content was measured by oven drying at 105°C until constant weight, while ash content was obtained by incineration at 550°C. Lipids were extracted using a Soxhlet apparatus with hexane for 8 h, and protein content was determined by the classical Kjeldahl method

(Lutz, 2008). Carbohydrates were quantified by difference, following the methodology described by Ogunlaja et al. (2020). The total energy value was estimated using the equation proposed by Palmeira et al. (2019):

Energy (kcal) = 4 × (g protein + g carbohydrates) + 9 × (g lipids)

2.7 Fourier transform-infrared (FT-IR) spectroscopy

The chemical profile of the samples was determined using a FTIR – ATR spectrophotometer (Agilent Cary 630) with attenuated total reflection module (FTIR-ATR) from 680 – 4000 cm^{-1}.

2.8 Scanning Electron Microscopy (SEM)

The Cacauí powders were characterized by Scanning Electron Microscopy (SEM) using a JSM-IT500HR electron microscope (JEOL, Tokyo, Japan), with a 30 kV electron beam and a magnification of 100×.

2.9 Thermogravimetric Analysis

The analysis was performed on a thermogravimetric analyzer (DTGA60 H, Shimadzu, Kyoto, Japan), operated under an inert nitrogen atmosphere at a flow rate of 20 mL/minute. In the analysis, 7.0 ± 1 mg of each sample were placed in an alumina crucible and heated to 900°C, with a heating rate of 10°C/minute.

2.10 Determination of macro- and microminerals by inductively cacauí seed powder optical emission spectroscopy (ICP-OES)

Acid digestion of 0.3 g of lyophilized sample was carried out using a microwave system MARS 6 (CEM Corporation, EUA) with 10 mL of ultrapure nitric acid (HNO_3). The digestion program consisted of a temperature ramp to 180°C within 15 min, followed by a holding time of 15 min and subsequent cooling to 70°C. After digestion, samples were quantitatively diluted to 25 mL with ultrapure water and stored at 4°C until analysis. Elemental quantification of macro- and microminerals was performed by inductively coupled plasma optical emission spectrometry (ICP-OES) using an Agilent 5800 system (Agilent Technologies), with argon as the nebulizer gas. Calibration curves were constructed using certified reference materials and exhibited excellent linearity ($R^2 > 0.999$), with relative standard errors (%RSE) below 10%, confirming the accuracy, sensitivity, and robustness of the analytical method (Mar et al., 2025). Limits of quantification (LOQ) were established based on calibration curves for each analite. For macrominerals, LOQ values were: K (766.491 nm, 0.5046 mg/L), Mg (279.553 nm, 1.012 mg/L), Ca (396.847 nm, 0.5072 mg/L), and P (213.618 nm, 0.0103 mg/L). For microminerals, LOQ values were: Ba (455.403 nm, 0.1034 mg/L), Cu (327.395 nm, 0.0052 mg/L), Fe (238.204 nm, 0.1027 mg/L), Mn (257.610 nm, 0.0824 mg/L), Ni (231.604 nm, 0.0104 mg/L), and Zn (213.857 nm, 0.0105 mg/L), demonstrating high analytical sensitivity across all elements. Method precision and accuracy were evaluated using procedural blanks and fortified samples prepared with standard solutions. The coefficient of variation (%CV) was ≤ 10% for all analytes, indicating excellent repeatability. Recovery values ranged from 85–

115% for spiked blanks and 82–114% for fortified samples, all within the acceptable range of 80–120%, thereby confirming the reliability and trueness of the method in accordance with Instituto Nacional de Metrologia, Qualidade e Tecnologia guidelines.

2.11 Statistical analysis

Statistical analysis was performed using analysis of variance (ANOVA) in R software (version 3.5.1). Differences among treatment means were evaluated by Tukey's test, with a significance level of 5% ($p \leq 0.05$).

3. Results and discussion

3.1 Effect of cold atmospheric plasma pretreatment on antioxidant activity

Table 1 presents the antioxidant activity of cacauí seed powder samples subjected to different ultrasound pretreatment conditions, evaluated using the DPPH, ABTS, and FRAP assays, as well as the total phenolic content (TPC). The results indicate that the ultrasonic treatment significantly influenced the antioxidant capacity of the samples, highlighting the role of acoustic cavitation in promoting the release of bioactive compounds from the plant matrix.

Table 1
Effect of ultrasound pretreatment on antioxidant capacity (DPPH, ABTS, FRAP) and total phenolic content of cacauí seed powders.

Samples	DPPH (μMTrolox/mL)	ABTS (μMTrolox/mL)	TPC (mgGAE/mL)	FRAP (μMFe(II)/mL)
B	825.2 ± 6.2^{g}	1074.1 ± 6.9^{g}	38.9 ± 1.1^{g}	920.6 ± 3.9^{g}
C20/4	761.0 ± 6.6^{h}	898.5 ± 10.1^{h}	22.1 ± 1.2^{h}	732.1 ± 1.7^{h}
C20/8	1299.3 ± 6.2^{c}	1834.1 ± 8.3^{c}	163.1 ± 5.5^{c}	1239.5 ± 1.7^{c}
C20/12	706.1 ± 6.2^{j}	834.1 ± 8.3^{i}	14.3 ± 0.8^{i}	698.7 ± 3.9^{i}
C40/4	582.7 ± 3.8^{i}	737.4 ± 8.3^{j}	10.9 ± 0.8^{j}	673.9 ± 3.6^{j}
C40/8	950.2 ± 6.2^{f}	1267.4 ± 10.1^{f}	85.0 ± 1.0^{f}	940.2 ± 2.9^{f}
C40/12	1501.8 ± 5.2^{b}	1966.3 ± 6.6^{b}	227.2 ± 0.7^{b}	1260.6 ± 3.9^{b}
C70/4	1080.2 ± 5.2^{e}	1438.5 ± 10.7^{e}	131.6 ± 0.5^{e}	1017.6 ± 1.7^{e}
C70/8	1105.2 ± 5.2^{d}	1561.8 ± 8.4^{d}	145.8 ± 1.0^{d}	1053.2 ± 2.8^{d}
C70/12	1549.3 ± 8.8^{a}	2035.2 ± 10.1^{a}	293.6 ± 0.9^{a}	1395.0 ± 2.8^{a}
B: control; CX/Y: X (20, 40, 70) thermal amplitude / Y (4, 8, 12) time.				

Samples subjected to higher amplitudes and longer processing times showed increased antioxidant activity and total phenolic content. The C70/12 condition presented the highest values for all evaluated parameters (DPPH = 1549.3 μM Trolox/mL; ABTS = 2035.2 μM Trolox/mL; TPC = 293.6 mg GAE/mL; FRAP = 1395.0 μM Fe(II)/mL), indicating that increasing ultrasound intensity enhances the extraction of phenolic compounds and other metabolites with reducing capacity. This behavior can be attributed to the cavitation phenomenon, in which the formation and collapse of microbubbles generate shear forces capable of disrupting cell walls and improving mass transfer between the solvent and intracellular compounds (Vilkhu et al., 2008).

Compared to the control sample (B), the ultrasound-treated samples showed that certain conditions resulted in a marked increase in antioxidant activity, particularly for C20/8 and C40/12, suggesting that there is an optimal combination of amplitude and processing time capable of maximizing the release of phenolic compounds. On the other hand, some lower-intensity treatments, such as C40/4 and C20/12, presented lower values than the control sample, indicating that shorter processing times or insufficient energy may not be enough to promote effective disruption of the cell matrix. Ultrasound-assisted extraction can significantly increase the yield of phenolic compounds in plant matrices due to the formation of microjets and shear forces that promote structural disintegration of the cell wall (Chemat et

al., 2017). Kumar et al. (2021) reported that increasing ultrasonic power enhances the extraction efficiency of phenolic compounds, an effect associated with the increase in particle surface area and improved solvent penetration into the plant matrix, thereby promoting the release of bioactive metabolites.

The total phenolic content showed a strong correlation with the antioxidant assay results, indicating that phenolic compounds are primarily responsible for the free radical scavenging activity. Phenolic compounds, such as flavonoids and phenolic acids, exhibit a high capacity for electron donation and radical stabilization due to the presence of conjugated aromatic ring structures (Shahidi & Ambigaipalan, 2015).

The FRAP assay showed a trend similar to the DPPH and ABTS methods, confirming that increasing ultrasound intensity enhanced the reducing capacity of the extracts. Studies have demonstrated that ultrasonic treatments can improve the reducing power of plant extracts due to the enhanced release of phenolic compounds bound to the lignocellulosic matrix (Vilkhu et al., 2008).

The results obtained demonstrate that ultrasound pretreatment is an effective strategy to enhance the availability of phenolic compounds and improve the antioxidant activity of cacauí seed powder. Studies involving plant matrices rich in polyphenols indicate that the application of ultrasound can significantly increase the yield of antioxidant compounds, enhancing their extraction without causing relevant chemical degradation, highlighting the potential of this technology as a promising approach for obtaining bioactive metabolites (Sun et al., 2011).

3.2 Theacrine mass spectrometric identification

The LC–ESI–QTOF-MS analysis of theacrine ($C_9H_{12}N_4O_3$) performed in positive ionization mode generated high-resolution mass spectral data, enabling reliable structural confirmation based on accurate mass determination and characteristic fragmentation pathways (Fig. 1). The protonated molecular ion $[M + H]^+$ was detected at m/z 225.0987, corresponding to the elemental composition $C_9H_{13}N_4O_3^+$, in excellent agreement with the theoretical exact mass (mass error, Δ = −0.4 ppm). The low mass deviation obtained confirms the high analytical accuracy of the QTOF system and supports the unequivocal identification of theacrine in the analyzed sample.

The fragmentation pattern was characterized by a prominent ion at m/z 210.0753, corresponding to the neutral loss of a methyl radical ($\bullet CH_3$, 15.0234 Da), yielding the ion $C_8H_{10}N_4O_3^+$ (Δ = 0.0 ppm). Further fragmentation of the protonated molecular ion led to the formation of m/z 168.0769, attributed to the neutral loss of a CNO moiety (41.9980 Da), corresponding to $C_7H_{10}N_3O_2^+$ (Δ = −2.3 ppm). Additionally, the fragment ion at m/z 153.0527 was observed and assigned to $C_6H_7N_3O_2^+$ (Δ = −7.2 ppm), resulting from a subsequent methyl radical loss from the ion at m/z 168.0769 (Fonseca Júnior et al., 2025).

The identity of theacrine in the sample was further confirmed by the injection of an authentic standard in the HPLC-DAD system, which exhibited identical retention time and a characteristic absorption band at 292 nm, consistent with the UV–Vis profile of theacrine.

The quantitative results demonstrated variation in theacrine concentration among samples subjected to different ultrasound amplitudes, indicating that acoustic energy significantly influences the extraction and availability of this alkaloid (Fig. 2). The sample treated with higher ultrasound amplitude (C70/12) showed increased theacrine content compared to the control and lower amplitude treatments, suggesting that cavitation phenomena promoted enhanced cell disruption and improved mass transfer of intracellular compounds. Ultrasound-assisted extraction has been widely reported as an efficient technique to increase recovery of alkaloids and other bioactive molecules due to mechanical effects such as microjet formation, shear forces and rupture of cell walls (Shen et al., 2023).

In contrast, the sample with lower theacrine concentration (C40/4) may indicate limited structural disruption of plant tissues, resulting in reduced release of intracellular metabolites. Lower ultrasound amplitude produces weaker cavitation intensity, which may not be sufficient to fully disrupt lignocellulosic structures that protect nitrogen-containing secondary metabolites. Studies demonstrate that ultrasound frequency and power directly influence cavitation bubble size and collapse intensity, thereby affecting extraction yield of alkaloids, phenolics and methylxanthine derivatives (Vardanega et al., 2014).

Previous research evaluating ultrasound-assisted extraction of bioactive compounds from plant matrices reported significant increases in yield when higher acoustic power or longer exposure times were applied. These effects are attributed to increased solvent penetration, improved diffusion kinetics and enhanced desorption of compounds bound to structural components such as cellulose and proteins. Similar behavior has been observed for caffeine and structurally related purine alkaloids, where ultrasound pretreatment improves extraction efficiency compared to conventional techniques (Zabot et al., 2021).

The higher concentration of theacrine observed in the sample treated at greater amplitude may also be related to partial modification of intermolecular interactions between alkaloids and macromolecules such as polysaccharides and proteins. Ultrasound treatment can weaken hydrogen bonding interactions and increase accessibility of compounds located within cellular compartments. Structural disruption observed in SEM images supports this interpretation, demonstrating increased porosity and reduced particle compactness in samples subjected to higher acoustic energy (Dzah et al., 2020).

Conversely, excessively intense ultrasound conditions may also promote degradation of thermolabile compounds depending on exposure time and energy density. However, the preservation of theacrine structure observed in chromatographic profiles suggests that the applied conditions did not induce significant chemical degradation, indicating that the selected parameters were adequate to maximize extraction efficiency while maintaining molecular integrity. Similar findings have been reported for ultrasound-assisted extraction of alkaloids in tea and guarana matrices (Panda & Manickam, 2019).

The results indicate that ultrasound frequency (amplitude) plays a decisive role in determining the concentration of theacrine, with higher acoustic energy favoring compound release due to intensified cavitation effects. These findings confirm the potential of ultrasound technology as an efficient strategy

to enhance recovery of purine alkaloids from plant matrices, contributing to optimization of extraction processes for functional ingredients derived from Amazonian species.

3.3 Proximate Composition

The proximate composition results indicate that cacauí seed powder presents low moisture content (2.31–3.98%), high lipid content (25.94–28.92%), moderate protein levels (14.69–16.25%), and predominance of carbohydrates (50.31–54.37%), in addition to mineral content (ash) ranging from 1.78 to 2.85%. These results highlight the nutritional and technological potential of this raw material, particularly for applications as a functional ingredient or source of bioactive compounds (Table 2).

Table 2
Proximate composition of the samples (%)

Sample	Moisture (%)	Ash (%)	Lipids (%)	Proteins (%)	Carbohydrates (%)
B	3.16 ± 0.01	2.66 ± 0.01	26.63 ± 0.01	14.89 ± 0.03	52.67 ± 0.03
C20/4	3.34 ± 0.01	2.41 ± 0.01	28.92 ± 0.02	15.01 ± 0.01	50.31 ± 0.02
C20/8	2.31 ± 0.01	2.33 ± 0.01	25.94 ± 0.01	15.05 ± 0.03	54.37 ± 0.01
C20/12	2.40 ± 0.02	2.27 ± 0.03	27.57 ± 0.01	16.25 ± 0.02	51.51 ± 0.00
C40/4	3.03 ± 0.03	1.78 ± 0.01	28.23 ± 0.01	15.53 ± 0.00	51.43 ± 0.03
C40/8	3.62 ± 0.01	2.16 ± 0.01	28.86 ± 0.03	14.69 ± 0.01	50.66 ± 0.04
C40/12	3.98 ± 0.01	2.37 ± 0.02	27.34 ± 0.02	14.98 ± 0.01	51.33 ± 0.03
C70/4	3.13 ± 0.02	2.43 ± 0.01	28.68 ± 0.01	15.32 ± 0.00	50.44 ± 0.02
C70/8	3.16 ± 0.01	2.57 ± 0.01	28.02 ± 0.01	15.29 ± 0.00	50.96 ± 0.01
C70/12	3.52 ± 0.02	2.85 ± 0.01	27.87 ± 0.01	15.02 ± 0.02	50.75 ± 0.03

Values are expressed as mean ± standard deviation (n = 3). Carbohydrates were calculated by difference.

The low moisture content observed in all samples is a positive factor for product stability, as it reduces water activity and, consequently, susceptibility to microbial growth and chemical degradation during storage. Studies on seeds from species of the genus *Theobroma* have shown that reduced moisture contributes to greater stability of phenolic and lipid compounds, preserving antioxidant and nutritional properties (Mar et al., 2024b).

The lipid content found in the samples (26–29%) is characteristic of seeds from the genus *Theobroma*, which present high concentrations of fatty acids, particularly oleic and stearic acids, associated with energy storage and relevant technological properties, such as texture and oxidative stability (Cerri et al., 2019). Similar lipid and protein values have been reported for cocoa seeds, indicating that these raw

materials have potential as a source of vegetable fat with applications in the food industry (Jean-Marie et al., 2022).

The protein content (14.69–16.25%) falls within the range reported for *Theobroma* seeds, which may present values close to 15% on a dry basis, contributing to the nutritional and functional value of the product (Osei et al., 2023). Proteins present in these seeds play an important role in metabolic processes and may contribute to technological properties, such as water retention and emulsification capacity in food systems.

The carbohydrate fraction was predominant (50–54%), indicating that the seed powder has potential as an energy source. The predominance of carbohydrates in plant matrices is also associated with the presence of structural fibers and polysaccharides that influence functional characteristics, such as water absorption capacity and stability of colloidal systems (Jean-Marie et al., 2022).

The ash content (1.78–2.85%) indicates the presence of minerals important for human metabolism and the nutritional value of the food. The mineral composition of species from the genus *Theobroma* includes essential elements such as potassium, magnesium, and iron, which contribute to functional and nutritional properties (Mar et al., 2024b).

It was observed that ultrasound pretreatment promoted slight variations in the chemical constituents of the samples. Ultrasound can induce structural modifications in the plant matrix, enhancing the release of intracellular compounds due to the cavitation phenomenon, which promotes cell wall disruption and increases the availability of bioactive compounds (Mar et al., 2024b). This behavior may explain the variations observed mainly in the lipid, protein, and carbohydrate contents among the different treatments (20, 40, and 70% amplitude and processing times of 4, 8, and 12 min).

The results demonstrate that cacauí seed powder presents a nutritional composition similar to that reported for other species of the genus, highlighting its potential as a promising source of lipids, proteins, and bioactive compounds with potential application in the functional food industry.

3.4 Fourier Transform Infrared Spectroscopy (FTIR)

Fourier transform infrared spectroscopy (FTIR) was used for the structural characterization of cacauí seed flour, enabling the identification of functional groups associated with the main chemical constituents of the sample.

The FTIR spectra (Fig. 3) showed characteristic bands of lipids, proteins, and carbohydrates, confirming the complex nature of the plant matrix. Bands observed in the region 2922–2914 cm^{-1} and 2855–2847 cm^{-1} are attributed to C–H stretching vibrations of aliphatic chains, typical of fatty acids and triglycerides present in lipid-rich seeds. Studies on cocoa have shown that peaks around 2920 and 2850 cm^{-1} are associated with lipids, olefins, and aromatic compounds formed during thermal processing (Collazos-Escobar et al., 2024).

The presence of an intense band at 1736 cm^{-1} is associated with the stretching vibration of the C = O bond of ester groups, indicating the presence of triacylglycerols and other structural lipid compounds. Similar results have been reported in FTIR analyses of cocoa and chocolate, where bands in the 1745–1730 cm^{-1} region were attributed to lipids and phenolic-derived compounds (I. A. Santos et al., 2021).

The band observed at approximately 1625 cm^{-1} is associated with the amide I vibration, corresponding to C = O stretching of proteins. This region may also indicate the presence of conjugated phenolic compounds and flavonoids, which are important for antioxidant activity. Studies have shown that peaks in the range of 1616–1690 cm^{-1} are related to the presence of proteins, phenolics, and Maillard reaction products in cocoa matrices.

The absorption near 1543 cm^{-1} corresponds to the amide II band, associated with N–H bending and C–N stretching vibrations of proteins. FTIR studies on cocoa beans report similar signals linked to aromatic compounds and protein structures that influence antioxidant and functional Properties (Oracz & Zyzelewicz, 2019).

In the region between 1148–991 cm^{-1}, the bands are attributed to C–O and C–O–C stretching vibrations, characteristic of polysaccharides, cellulose, and hemicellulose present in the plant cell wall. Studies indicate that carbohydrates such as glucose, fructose, and sucrose exhibit typical absorptions between 1400 and 900 cm^{-1}, and this region is frequently associated with the structural matrix of cocoa beans and seeds (Collazos-Escobar et al., 2024).

Comparing the ultrasonic treatments (20, 40, and 70% amplitude), small variations in band intensity can be observed, suggesting structural modifications induced by acoustic cavitation. Ultrasound treatment can promote cell wall disruption and modify intermolecular interactions, increasing the exposure of phenolic compounds and proteins without drastically altering the main functional groups. FTIR spectroscopy has been widely used to monitor structural changes in cocoa and its derivatives, demonstrating sensitivity to modifications caused by thermal and mechanical processing (Küçükduman et al., 2026).

Ultrasound pre-treatment promoted subtle structural modifications in the chemical matrix of cacauí seed powder, while preserving the main functional groups associated with lipids, proteins, and carbohydrates. This behavior is consistent with studies showing that emerging processing techniques can enhance the availability of bioactive compounds without causing significant chemical degradation.

3.4 Scanning electron microscopy (SEM)

Scanning electron microscopy (SEM) micrographs (Fig. A–J) reveal significant morphological differences between the untreated sample and those subjected to ultrasound pre-treatment at different amplitudes (20, 40, and 70%) and processing times (4, 8, and 12 min). The structural modifications observed in the particles indicate that acoustic cavitation promoted progressive disruption of the plant matrix, which may influence the extraction of bioactive compounds and the functional properties of the powder.

The untreated sample (Fig. A – control) exhibits particles with irregular geometry, a relatively compact structure, and smooth surfaces, typical of plant matrices rich in lipids and polysaccharides. Similar morphologies have been reported for cocoa powder and other *Theobroma* species, which commonly present agglomerated particles due to interactions between lipids and proteins, forming cohesive structures (Rajewska & Mierzwa, 2017).

After ultrasound treatment at 20% amplitude (Fig. B–D), structural modifications become evident. Sample C20/4 (Fig. B) shows the onset of surface roughness and partial particle fragmentation. At longer processing times, C20/8 and C20/12 (Fig. C and D) exhibit increased irregularity, pore formation, and partial disintegration of agglomerates. Ultrasonic waves generate cavitation bubbles that collapse near the particle surface, producing localized high pressure and temperature, which promotes cell wall disruption and increases porosity (Umaña et al., 2022).

For treatments at 40% amplitude (Fig. E–G), structural disruption becomes more pronounced. The particles appear less compact and more fragmented, indicating greater mechanical stress promoted by ultrasonic energy. The formation of fissures and irregular surfaces suggests structural weakening of the cellular matrix. Studies have shown that ultrasound processing can significantly modify plant microstructure, promoting the rupture of parenchymal cells and facilitating solvent penetration (Khadhraoui et al., 2018).

At 70% amplitude (Fig. H–J), more intense morphological changes are observed, characterized by greater fragmentation, rougher surfaces, and a reduction in particle size. The C70/12 sample (Fig. J) shows clear structural collapse and the formation of smaller aggregates, indicating a higher intensity of cavitation effects. According to Prempeh et al. (2025), higher ultrasound amplitudes increase shear forces and microjet formation, promoting disruption of plant tissues and enhancing the release of intracellular compounds such as phenolics and lipids.

The progressive increase in structural disorganization observed with increasing amplitude and processing time confirms that ultrasound affects the integrity of the plant matrix. A similar behavior has been reported for *Pouteria lucuma* seeds, where ultrasound treatment promoted particle size reduction and increased surface area, improving the extraction efficiency of bioactive compounds (Orizano-Ponce et al., 2025).

The morphological changes observed in the SEM images are consistent with the FTIR and antioxidant results, suggesting that ultrasound promoted structural modifications capable of increasing the accessibility of phenolic compounds. Prempeh et al. (2025) reported that the development of porous structures and the reduction in particle size can enhance solvent penetration and improve mass transfer efficiency during extraction processes, thereby facilitating the release of intracellular compounds.

3.5 Thermogravimetric analysis

The TG and DTG curves showed a degradation profile typical of lignocellulosic biomasses and oilseed matrices, characterized by three main stages of mass loss associated with moisture evaporation and

decomposition of structural macromolecules (Fig. 5). Similar thermal behavior has been reported for cocoa by-products, which present complex matrices composed of lipids, proteins, cellulose, and lignin (Londoño-Larrea et al., 2022).

The first degradation stage, observed between approximately 25 and 150°C, showed mass losses ranging from 4.29 to 8.38%, corresponding to the evaporation of free and bound water, as well as low molecular weight volatile compounds. The reduction in mass loss observed in ultrasound-treated samples, particularly C20/12 and C70/12, suggests modifications in water retention capacity, possibly due to microstructural disruption caused by cavitation effects. Similar results have been reported for plant biomasses subjected to physical pretreatments, in which structural modifications reduced hydrogen bonding interactions between water molecules and polysaccharides (Soares & Oliveira, 2022).

The second stage of thermal degradation, occurring between 130 and 430°C, corresponded to the main mass loss event (approximately 68–71%) and is associated with the decomposition of hemicellulose, cellulose, proteins, and lipids. The DTG peaks observed between 280 and 350°C indicate maximum degradation rates of these macromolecules, consistent with thermal profiles reported for cocoa shells, cupuaçu seeds, and other lignocellulosic materials (Benítez et al., 2023).

The third degradation stage, observed between 420 and 900°C, with mass losses ranging from 17.77 to 20.50%, is associated with lignin decomposition and the formation of carbonaceous residues. Lignin exhibits high thermal stability due to its complex aromatic structure, resulting in gradual degradation over a wide temperature range (Gangil, 2014). The slightly lower mass loss observed for sample C70/12 suggests greater thermal stability, possibly related to structural rearrangements promoted by the ultrasonic treatment. Similar behavior has been observed in oilseed cakes and cocoa residues, where physical pretreatments influence pyrolysis pathways and char formation (Rojas et al., 2023).

Ultrasound treatment at 70% amplitude for 12 minutes promoted the greatest structural modification, reflected by increased particle irregularity and a slight improvement in thermal stability in the final degradation phase. The combined analytical approach confirms that cavitation effects modify the organization of the lignocellulosic matrix, facilitating heat transfer and altering degradation intensity, while preserving the chemical integrity of the material. These findings suggest that ultrasound pretreatment represents a promising strategy to modify the physicochemical properties of cacauí seed powder, potentially improving its applicability in food, pharmaceutical, and biotechnological processes.

3.6 Determination of macro- and microminerals by inductively cacauí seed powder optical emission spectroscopy (ICP-OES)

The mineral composition of cacauí seed powder showed predominance of macronutrients such as potassium (K), phosphorus (P), magnesium (Mg), and calcium (Ca), which are commonly reported as the main inorganic constituents of seeds from the *Theobroma* genus (Fig. 6). These minerals perform important physiological functions in plant metabolism and contribute to the nutritional value of products

derived from cacauí. Previous studies indicate that cocoa beans contain significant amounts of K, Mg, and P, which are associated with enzymatic activation, osmotic regulation, and structural stability of cellular components (Ponce et al., 2021).

Studies evaluating the mineral composition of cocoa cultivated under different soil conditions have reported strong correlations among K, Ca, P, and Mg concentrations, demonstrating that mineral accumulation depends on both genotype and environmental factors (de Araujo et al., 2017). Cocoa and cupuaçu seeds have been described as important dietary sources of Mg, Fe, and Zn, minerals associated with antioxidant defense systems and maintenance of metabolic homeostasis. In addition, these micronutrients contribute to functional properties and technological stability of plant-derived ingredients (Jean-Marie et al., 2022).

Trace elements such as iron (Fe), zinc (Zn), manganese (Mn), and copper (Cu) were also detected (Fig. 7), demonstrating similarity with mineral profiles reported for cocoa beans subjected to fermentation and processing. These micronutrients act as cofactors of antioxidant enzymes, including superoxide dismutase and catalase, which play important roles in controlling oxidative reactions in plant tissues and food matrices. Studies indicate that fermentation and post-harvest treatments may influence mineral bioavailability, particularly Fe and Zn, without significantly altering total mineral concentrations (Millena et al., 2023).

The mineral profile observed in cacao-related seeds is consistent with reports describing *Theobroma cacao* as an important source of essential macro- and microelements, including Ca, Mg, Zn, and Cu, which contribute to nutritional quality and potential functional benefits. Variability in mineral composition may be associated with soil characteristics, genetic factors, and environmental conditions during plant development. Furthermore, the accumulation of trace elements in cocoa plants has been shown to depend on mineral availability in the soil and plant uptake mechanisms (Lewis et al., 2021).

The mineral composition of cacauí seed powder reinforces the nutritional potential of Amazonian *Theobroma* species as sources of essential elements relevant to human health and food applications. Similar mineral distributions have been reported in cocoa and cupuaçu seeds, highlighting the technological and nutritional value of these varieties (Gattward et al., 2012).

4. Conclusions

Ultrasound pre-treatment effectively modified the structural, chemical, and functional properties of cacauí seed powder without causing significant chemical degradation. FTIR confirmed typical functional groups, while SEM revealed increased porosity and cell wall disruption, enhancing the accessibility of phenolic compounds. The identification of theacrine highlights the potential of cacauí as a source of bioactive alkaloids with stimulant and antioxidant properties. Thermogravimetric analysis showed that the treatment preserved thermal stability. The highest intensity condition (70% amplitude for 12 minutes) resulted in greater total phenolic content and antioxidant activity, indicating improved release of bioactive metabolites. Additionally, the proximate composition and mineral profile demonstrated the high

nutritional value of cacauí. Overall, ultrasound is a promising technology for improving the extraction of bioactive compounds and the functional properties of Amazonian raw materials for food, pharmaceutical, and biotechnological applications.

Declarations

Conflicts of Interest:

The authors declare no conflict of interest.

Clinical trial number

Not applicable.

Ethics Approval:

Not applicable

Consent to Participate:

Not applicable

Consent to Publish:

Not applicable

Declaration of Use of Artificial Intelligence

During the preparation of this manuscript, the authors used ChatGPT (OpenAI, GPT-4o, version accessed in March 2026) for orthographic and grammatical revision of the text. After using this tool, the authors thoroughly reviewed and edited the content and assume full responsibility for the final version of the manuscript.

Ethics approval and consent to participate

The plant material used in this study consisted of cacauí seeds (*Theobroma speciosum* Willd. ex Spreng), of cultivated origin, obtained at km 14 in the municipality of Careiro Castanho, Amazonas, Brazil. All applicable ethical and legal guidelines were followed, and the study was duly registered in the National System for the Management of Genetic Heritage and Associated Traditional Knowledge (SisGen) under registration number A9F3E4F. As the material was cultivated, no specific authorization or permits for collection from wild populations were required. The botanical identification of the species was carried out by Valdely Ferreira Kinupp. A voucher specimen was deposited in a publicly accessible collection at the Herbarium of the Federal Institute of Education, Science and Technology of Amazonas (EAFM), under voucher number EAFM nº 17.682, ensuring traceability and access to the material for future reference.

Contributions

Conceptualization: JMM and JdeAB; Methodology: JMM, DdeQR, CMR, FJM, DNM and VFK; Investigation: JMM, DdeQR, AdeSC, EOdosS and FdasCdoA; Data Curation: JMM, DdeQR, AdeSC and JdeAB; Writing—original draft preparation: JMM and DdeQR; Writing—review and editing: JMM, JdeAB, EAS, PHC and RFC. Visualization: JdeAB, EAS and PHC

Funding Statement:

The authors declare that this work received no financial support from public, private, or non-profit funding agencies.

Author Contribution

Conceptualization: JMM and JdeAB; Methodology: JMM, DdeQR, CMR, FJM, DNM and VFK; Investigation: JMM, DdeQR, AdeSC, EOdosS and FdasCdoA; Data Curation: JMM, DdeQR, AdeSC and JdeAB; Writing—original draft preparation: JMM and DdeQR; Writing—review and editing: JMM, JdeAB, EAS, PHC and RFC. Visualization: JdeAB, EAS and PHC

Acknowledgement

The authors gratefully acknowledge the financial support provided by the Conselho Nacional de Desenvolvimento Científico e Tecnológico (CNPq) and Coordenação de Aperfeiçoamento de Pessoal de Nível Superior (CAPES) for funding and fellowships. The authors also thank the Fundação de Amparo à Pesquisa do Estado do Amazonas (FAPEAM), through the Support Program for Stricto Sensu Graduate Studies (POSGRAD), for the scholarship granted. The authors acknowledge the Analytical Centers at Instituto Federal do Amazonas – Campus Manaus Centro (IFAM-CMC) and Universidade Federal do Amazonas (UFAM) for providing laboratory infrastructure. Additional analytical support and facilities were provided by the Biomolecule Purification Laboratory of the Multidisciplinary Support Center and the Chemical Analytical Center at UFAM, as well as the Samsung SRBR WTS Laboratory and the Laboratório de Pesquisas e Ensaios de Combustíveis (UFAM). The authors thank the Multiuser Center for the Analysis of Biomedical Phenomena of the Universidade do Estado do Amazonas (CMABio) for the scanning electron microscopy (SEM) analyses. The authors would like to thank Ms. Zaira Malheiros for providing the seed powders of Theobroma speciosum.

Data Availability

The datasets used and/or analysed during the current study are available from the corresponding author on reasonable request.

References

1. Benítez V, Rebollo-Hernanz M, Braojos C, Cañas S, Gil-Ramírez A, Aguilera Y, Martín-Cabrejas MA. Changes in the cocoa shell dietary fiber and phenolic compounds after extrusion determine its functional and physiological properties. Curr Res Food Sci. 2023;6:1–12. https://doi.org/10.1016/j.crfs.2023.100516.
2. Bento NA, Crispim M, dos Santos Lima A, Silva TC, da Silva Cruz L, da Silva GKP, Ionta M, Ferreira-Silva GÁ, dos Anjos Cruz JM, de Queiroz Rocha D. Araújo Bezerra, J, & Azevedo, L (2026) Bioprospecting of the Amazonian mapati fruit (*Pourouma cecropiifolia* Martius): Antiproliferative and antimalarial potential of peel and seed hydroethanolic extracts. Food Research International 228: 118297. https://doi.org/10.1016/j.foodres.2025.118297
3. Cerri M, Reale L, Zadra C. Metabolite Storage in *Theobroma cacao* L. Seed: cyto-histological and phytochemical analyses. Front Plant Sci. 2019;10:1–11. https://doi.org/10.3389/fpls.2019.01599.
4. Chemat F, Rombaut N, Sicaire AG, Meullemiestre A, Fabiano-Tixier AS, Abert-Vian M. Ultrasound assisted extraction of food and natural products. Mechanisms, techniques, combinations, protocols and applications. Rev Ultrason Sonochemistry. 2017;34:540–60. https://doi.org/10.1016/j.ultsonch.2016.06.035.
5. Collazos-Escobar GA, Barrios-Rodríguez YF, Bahamón-Monje AF, Gutiérrez-Guzmán N. Mid-infrared spectroscopy and machine learning as a complementary tool for sensory quality assessment of roasted cocoa-based products. Infrared Phys Technol. 2024;141:1–10. https://doi.org/10.1016/j.infrared.2024.105482.
6. de Araujo QR, Baligar VC, Loureiro GAHA, de Souza Júnior JO, Comerford NB. Impact of soils and cropping systems on mineral composition of dry cacao beans. J Soil Sci Plant Nutr. 2017;17:410–28. https://doi.org/10.4067/S0718-95162017005000030.
7. Dzah CS, Duan Y, Zhang H, Wen C, Zhang J, Chen G, Ma H. The effects of ultrasound assisted extraction on yield, antioxidant, anticancer and antimicrobial activity of polyphenol extracts: A review. Food Bioscience. 2020;35:100547. https://doi.org/10.1016/j.fbio.2020.100547.
8. da Fonseca Júnior EQ, de Rocha Q, Souza Coelho Oliveira D, Oliveira da Silva E, Amaral Souza S, Furlaneto F, da Silva Cruz G, Azevedo L, Frota L, Corrêa R, Sanches A, Campelo E. P. H., & de Araújo Bezerra, J. (2025). Chemical characterization, nutritional profile, and cytotoxicity potential of Amazonian *Theobroma sylvestre* Mart. fruits. Food Bioscience 73: 107673. https://doi.org/10.1016/j.fbio.2025.107673
9. Gangil S. Dominant thermogravimetric signatures of lignin in cashew shell as compared to cashew shell cake. Bioresour Technol. 2014;155:15–20. https://doi.org/10.1016/j.biortech.2013.12.087.
10. Gattward JN, Almeida AAF, Souza JO, Gomes FP, Kronzucker HJ. Sodium-potassium synergism in *Theobroma cacao*: Stimulation of photosynthesis, water-use efficiency and mineral nutrition. Physiol Plant. 2012;146:350–62. https://doi.org/10.1111/j.1399-3054.2012.01621.x.
11. González-Silva N, Nolasco-González Y, Aguilar-Hernández G, Sáyago-Ayerdi SG, Villagrán Z, Acosta JL, Montalvo-González E, Anaya-Esparza LM. Ultrasound-assisted extraction of phenolic

compounds from *Psidium cattleianum* leaves: optimization using the response surface methodology. Molecules. 2022;27:1–16. https://doi.org/10.3390/molecules27113557.

12. Jean-Marie E, Jiang W, Bereau D, Robinson JC. *Theobroma cacao* and *Theobroma grandiflorum*: botany, composition and pharmacological activities of pods and seeds. Foods. 2022;11:1–23. https://doi.org/10.3390/foods11243966.
13. Khadhraoui B, Turk M, Fabiano-Tixier AS, Petitcolas E, Robinet P, Imbert R, Maâtaoui ME, Chemat F. Histo-cytochemistry and scanning electron microscopy for studying spatial and temporal extraction of metabolites induced by ultrasound. Ultrason Sonochem. 2018;42:482–92. https://doi.org/10.1016/j.ultsonch.2017.11.029.
14. Küçükduman Y, Korkmaz İD, Çiftçi HG, Argün S, Bilge Özel G, Taştan Ülkü Ö, Toker ÖS, Mutlu Z. Monitoring of cocoa quality and conching, tempering, cooling processes in chocolate production with FTIR spectroscopy. J Food Meas Charact. 2026;20:1–12. https://doi.org/10.1007/s11694-025-03986-0.
15. Kumar K, Srivastav S, Singh V. Ultrasound assisted extraction (UAE) of bioactive compounds from fruit and vegetable processing by-products: A review. Ultrason - Sonochemistry. 2021;70:105325. https://doi.org/10.1016/j.ultsonch.2020.105325.
16. Lewis C, Lennon AM, Eudoxie G, Sivapatham P, Umaharan P. Plant metal concentrations in *Theobroma cacao* as affected by soil metal availability in different soil types. Chemosphere. 2021;262:127749. https://doi.org/10.1016/j.chemosphere.2020.127749.
17. Londoño-Larrea P, Villamarin-Barriga E, García AN, Marcilla A. Study of cocoa pod husks thermal decomposition. Appl Sci (Switzerland). 2022;12:15. https://doi.org/10.3390/app12189318.
18. Mar JM, Carolino AS, Neves KOG, Corrêa RF, Machado MB, Rocha, Dde Q, Kinupp VF, Sanches EA, Campelo PH, Bezerra JA. Enhancing the extraction efficiency of beneficial compounds from *Tapirira guianensis* fruit using ultrasound-assisted extraction and choline chloride deep eutectic solvent. Food Sci Technol. 2025;45:1–8. https://doi.org/10.5327/fst.493.
19. Mar JM, da Fonseca Júnior EQ, Corrêa RF, Campelo PH, Sanches EA, Bezerra JA. Theobroma spp.: A review of it's chemical and innovation potential for the food industry. Food Chem Adv. 2024;4:1–17. https://doi.org/10.1016/j.focha.2024.100683.
20. Mar JM, Frota R, Ramos S, Kinupp VF, Sanches EA, Campelo PH, Bezerra JA. Enhancing Bioactive compound bioaccessibility in *Tapirira guianensis* juices through ultrasound-assisted applications. Process. 2023;11:1–16. https://doi.org/10.3390/pr11092718.
21. Mar JM, Souza L, Picanço W, Bezerra A. Edible flowers from T*heobroma speciosum*: Aqueous extract rich in antioxidant compounds. Food Chem. 2021;356:129723. https://doi.org/10.1016/j.foodchem.2021.129723.
22. Millena CG, Balonzo ARR, Rentoy JR, Ruivivar SS, Bobiles SC. Effect of fermentation stages on the nutritional and mineral bioavailability of cacao beans (*Theobroma cacao* L). J Food Compos Anal. 2023;115:104886. https://doi.org/10.1016/j.jfca.2022.104886.

23. Ogunlaja OO, Moodley R, Baijnath H, Jonnalagadda SB. Elemental distribution and health risk assessment of the edible fruits of two ficus species, *Ficus sycomorus* L. and *Ficus burtt-davyi* Hutch. Biol Trace Elem Res. 2020;198:303–14. https://doi.org/10.1007/s12011-020-02048-4.
24. Oracz J, Zyzelewicz D. In vitro antioxidant activity and ftir characterization of high-molecular weight melanoidin fractions from different types of cocoa beans. Antioxidants. 2019;8:1–16. https://doi.org/10.3390/antiox8110560.
25. Orizano-Ponce E, Santillan G, Chamorro-Gómez RE, Villanueva-Tiburcio JE, Estacio-Laguna R, Cueto-Rosales CR, Palma-Lozano D, Cámara F, Cano D. Effect of ultrasound on the physical, morphological, and mechanical properties of bioplastic obtained from lucuma seed starch (*Pouteria lucuma*). Appl Food Res. 2025;5:1–11. https://doi.org/10.1016/j.afres.2025.100990.
26. Osei PA, Kpodo FM, Tettey CO, Dzah CS, Agbenorhevi JK, Hunkpe G, Nanga S. Proximate composition, phenolic, and antioxidant properties of soursop fruit parts. CYTA - J Food. 2023;21:475–80. https://doi.org/10.1080/19476337.2023.2227250.
27. Palmeira L, Pereira C, Dias MI, Abreu RMV, Corrêa RCG, Pires TCSP, Alves MJ, Barros L, Ferreira ICFR. Nutritional, chemical and bioactive profiles of different parts of a Portuguese common fig (*Ficus carica* L.) variety. Food Res Int. 2019;126:108572. https://doi.org/10.1016/j.foodres.2019.108572.
28. Panda D, Manickam S. Cavitation technology-the future of greener extraction method: A review on the extraction of natural products and process intensification mechanism and perspectives. Appl Sci (Switzerland). 2019;9:1–21. https://doi.org/10.3390/app9040766.
29. Ponce J, María S, Zurita G, Peñuela MC. Reproductive ecology of white cacao (*Theobroma bicolor* Humb. & Bonpl.) in Ecuador, western Amazonia: floral visitors and the impact of fungus and mistletoe on fruit production. Brazilian J Bot. 2021;44:479–89. https://doi.org/10.1007/s40415-021-00709-9.
30. Prempeh NYA, Nunekpeku X, Murugesan A, Li H. (2025) Ultrasound in the Food Industry: Mechanisms and Applications for Non-Invasive Texture and Quality Analysis. In Foods, 14: 1–16. https://doi.org/10.3390/foods14122057
31. Rajewska K, Mierzwa D. Influence of ultrasound on the microstructure of plant tissue. Innovative Food Sci Emerg Technol. 2017;43:117–29. https://doi.org/10.1016/j.ifset.2017.07.034.
32. Rojas M, Ruano D, Orrego-Restrepo E, Chejne F. Non-isothermal kinetics of cellulose, hemicellulose, and lignin degradation during cocoa bean shell pyrolysis. Biomass Bioenergy. 2023;177:106932. https://doi.org/10.1016/j.biombioe.2023.106932.
33. Santos IA, Conceição DG, Viana MB, Silva GJ, Santos LS, Ferrão SPB. NIR and MIR spectroscopy for quick detection of the adulteration of cocoa content in chocolates. Food Chem. 2021;349:1–6. https://doi.org/10.1016/j.foodchem.2021.129095.
34. Santos NC, Almeida RLJ, Albuquerque JC, de Andrade EWV, Gregório MG, Santos RMS, Rodrigues TJA, Carvalho RO, Gomes MMA, Moura HV, de Figueiredo DVP, Araújo MA, Lima, VRdo N, Mota MMA. Optimization of ultrasound pre-treatment and the effect of different drying techniques on

antioxidant capacity, bioaccessibility, structural and thermal properties of purple cabbage. Chem Eng Process - Process Intensif. 2024;201:1–12. https://doi.org/10.1016/j.cep.2024.109801.

35. Shahidi F, Ambigaipalan P. Phenolics and polyphenolics in foods, beverages and spices: Antioxidant activity and health effects - A review. J Funct Foods. 2015;18:820–97. https://doi.org/10.1016/j.jff.2015.06.018.
36. Shen L, Pang S, Zhong M, Sun Y, Qayum A, Liu Y, Rashid A, Xu B, Liang Q, Ma H, Ren X. A comprehensive review of ultrasonic assisted extraction (UAE) for bioactive components: Principles, advantages, equipment, and combined technologies. Ultrason Sonochem. 2023;101:106646. https://doi.org/10.1016/j.ultsonch.2023.106646.
37. Soares TF, Oliveira MBPP. Cocoa By-Products: Characterization of Bioactive Compounds and Beneficial Health Effects. Molecules. 2022;27:1–23. https://doi.org/10.3390/molecules27051625.
38. Sun Y, Liu Z, Wang J. Ultrasound-assisted extraction of five isoflavones from *Iris tectorum* Maxim. Sep Purif Technol. 2011;78:49–54. https://doi.org/10.1016/j.seppur.2011.01.017.
39. Umaña M, Calahorro M, Eim V, Rosselló C, Simal S. Measurement of microstructural changes promoted by ultrasound application on plant materials with different porosity. Ultrason Sonochem. 2022;88:106087. https://doi.org/10.1016/j.ultsonch.2022.106087.
40. Vardanega R, Santos DT, De Almeida MA. Intensification of bioactive compounds extraction from medicinal plants using ultrasonic irradiation. Pharmacogn Rev. 2014;8:88–95. https://doi.org/10.4103/0973-7847.134231.
41. Vilkhu K, Mawson R, Simons L, Bates D. Applications and opportunities for ultrasound assisted extraction in the food industry - A review. Innovative Food Sci Emerg Technol. 2008;9:161–9. https://doi.org/10.1016/j.ifset.2007.04.014.
42. Yusoff IM, Mat Taher Z, Rahmat Z, Chua LS. A review of ultrasound-assisted extraction for plant bioactive compounds: Phenolics, flavonoids, thymols, saponins and proteins. Food Res Int. 2022;157:111268. https://doi.org/10.1016/j.foodres.2022.111268.
43. Zabot GL, Viganó J, Silva EK. Low-frequency ultrasound coupled with high-pressure technologies: Impact of hybridized techniques on the recovery of phytochemical compounds. Molecules. 2021;26:1–20. https://doi.org/10.3390/molecules26175117.

Figures

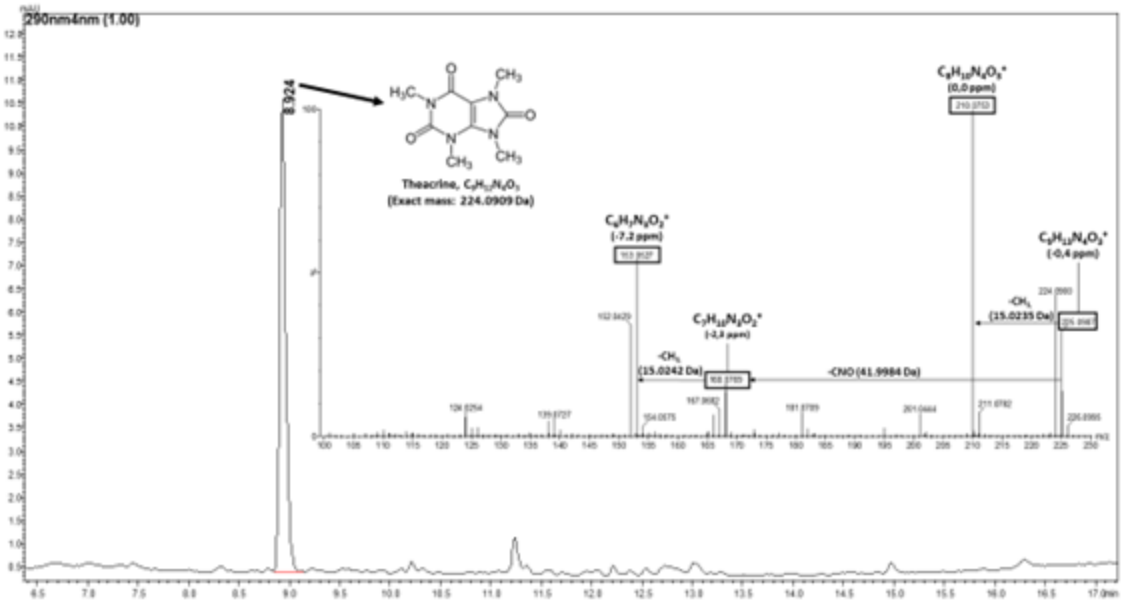

Figure 1

High-resolution ESI(+)-QTOF mass spectrum of theacrine, highlighting the protonated molecular ion and main fragment ions formed via sequential neutral losses

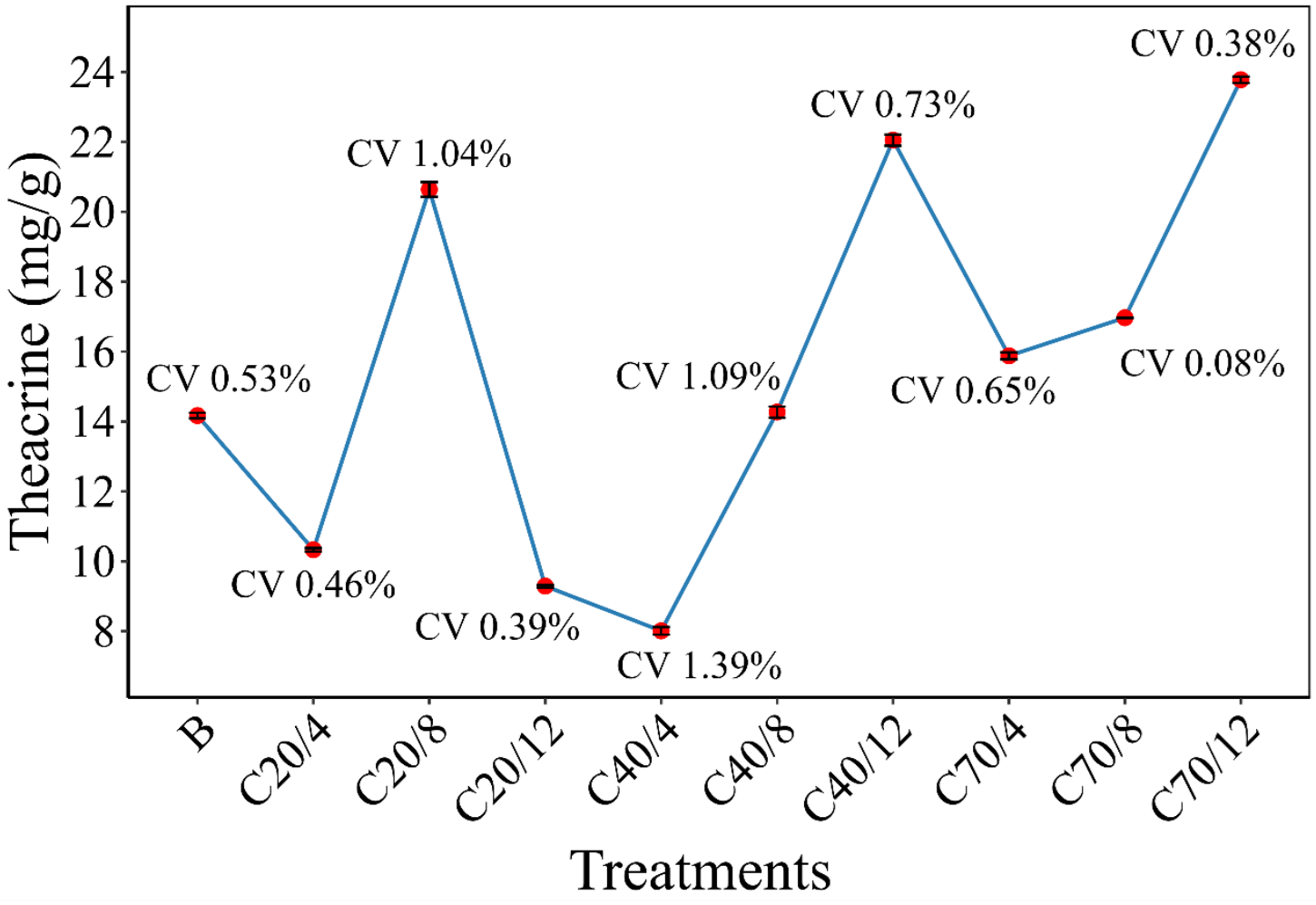

Figure 2

Comparison of theacrine concentration in samples treated with different ultrasound amplitudes (20, 40 and 70%) for 12 min determined by LC–ESI–QTOF-MS.

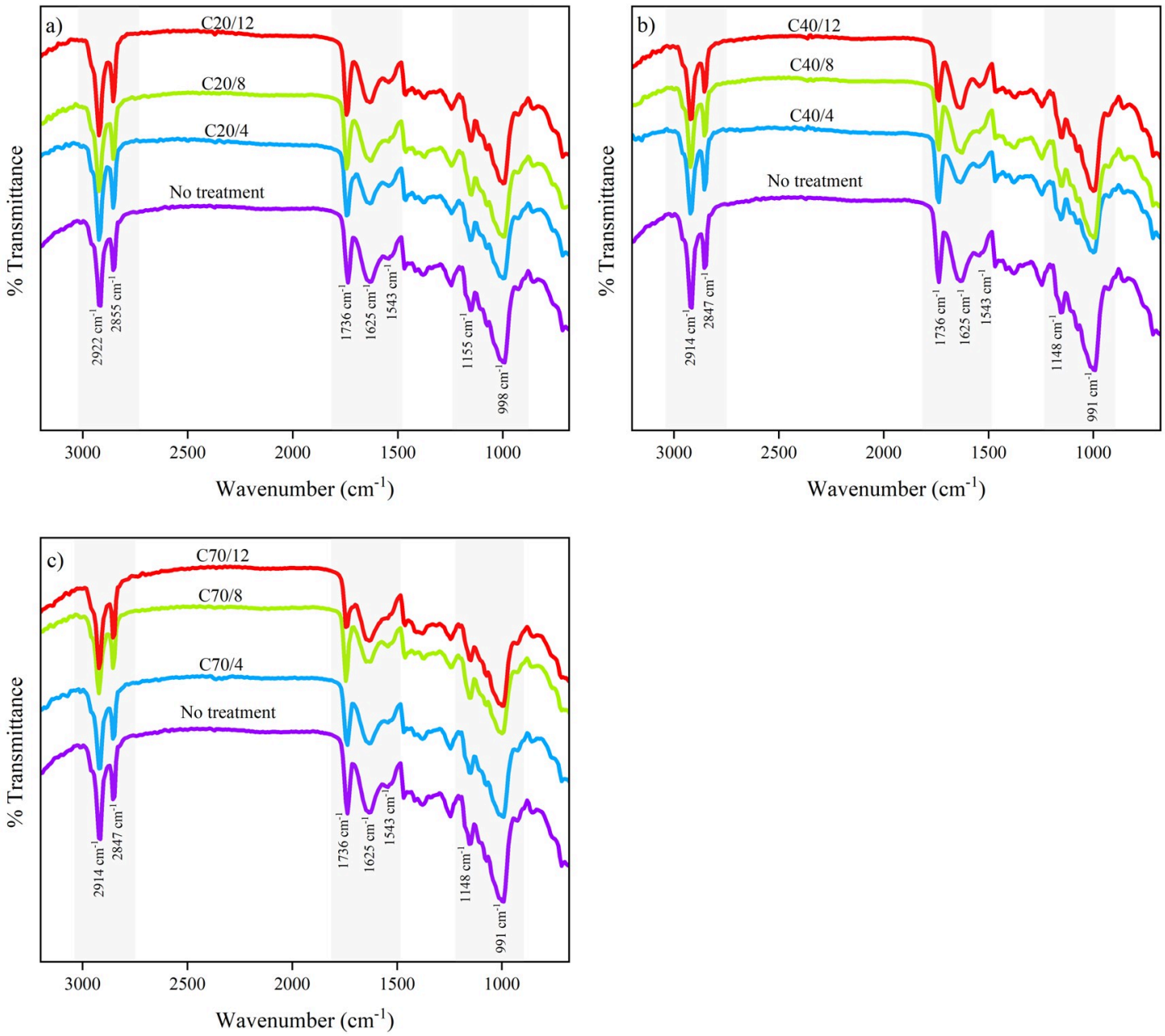

Figure 3

Fourier transform infrared spectroscopy (FTIR) of cacauí seed flour

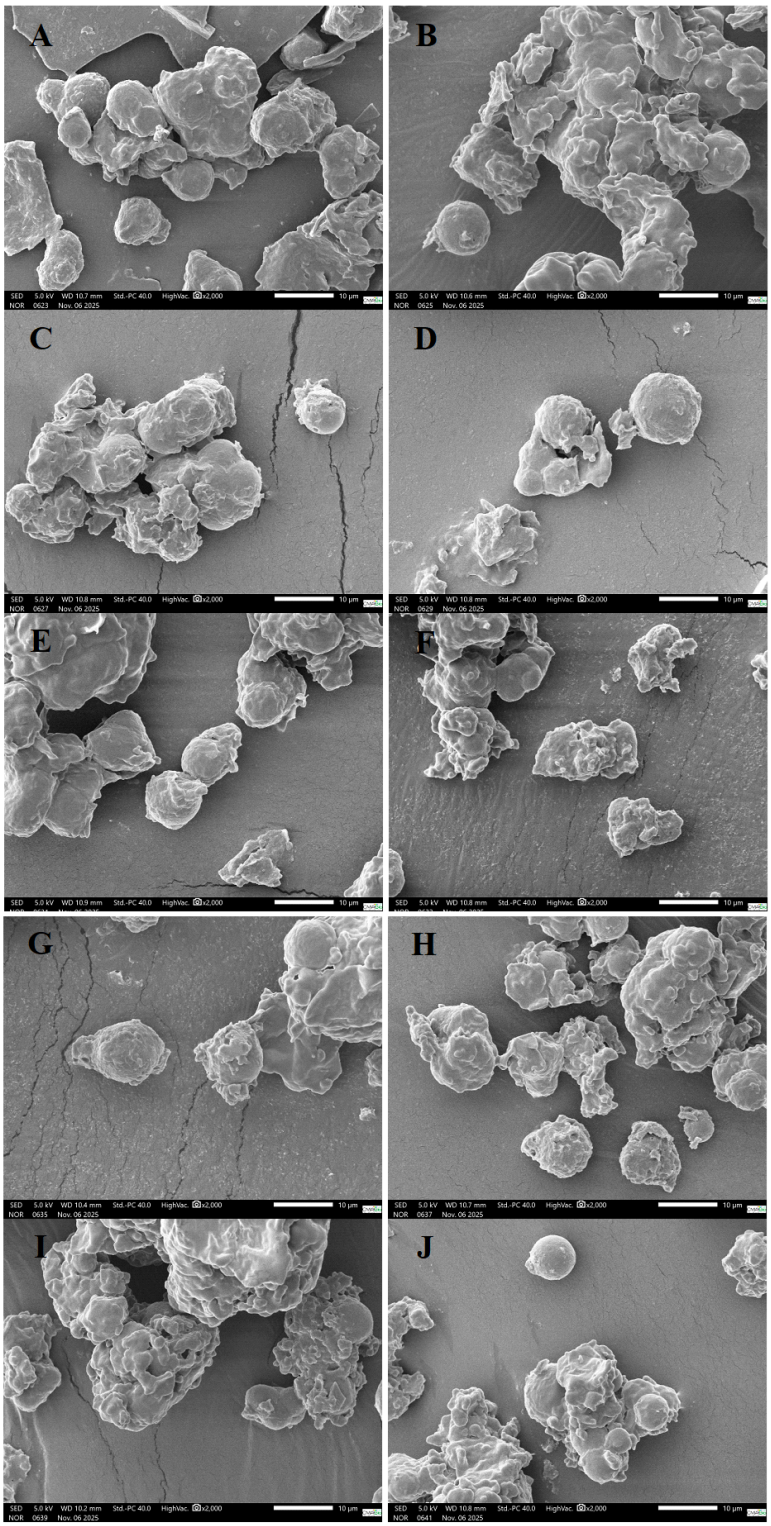

Figure 4

Scanning electron microscopy (SEM) micrographs of cacauí seed powder subjected to ultrasound pre-treatment

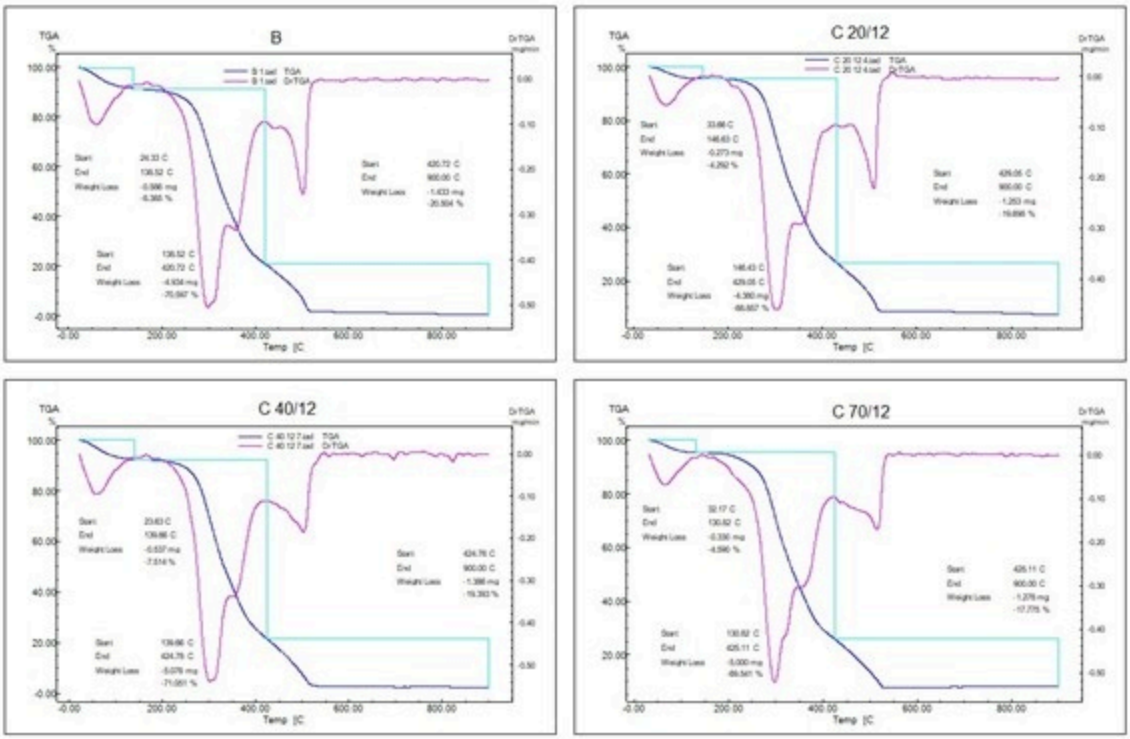

Figure 5

Thermogravimetric (TG) and derivative thermogravimetric (DTG) curves of cacauí seed powder: control sample (B) and ultrasound-treated samples at amplitudes of 20, 40 and 70% for 12 min.

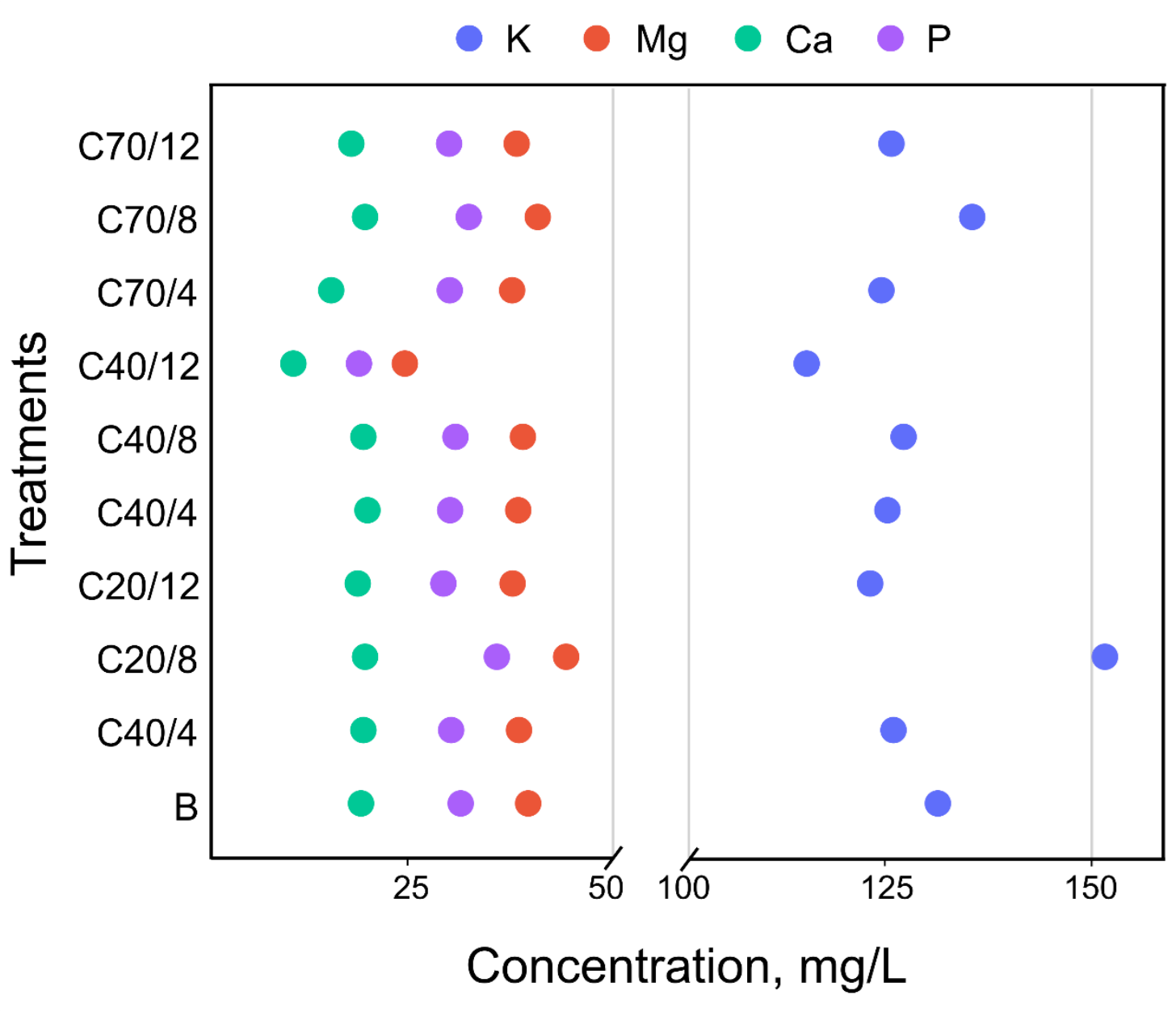

Figure 6

Macromineral composition (K, P, Ca, Mg and Na) of seed powder subjected to ultrasound pretreatment at different amplitudes (20, 40 and 70%) for 12 min, compared with the control sample.

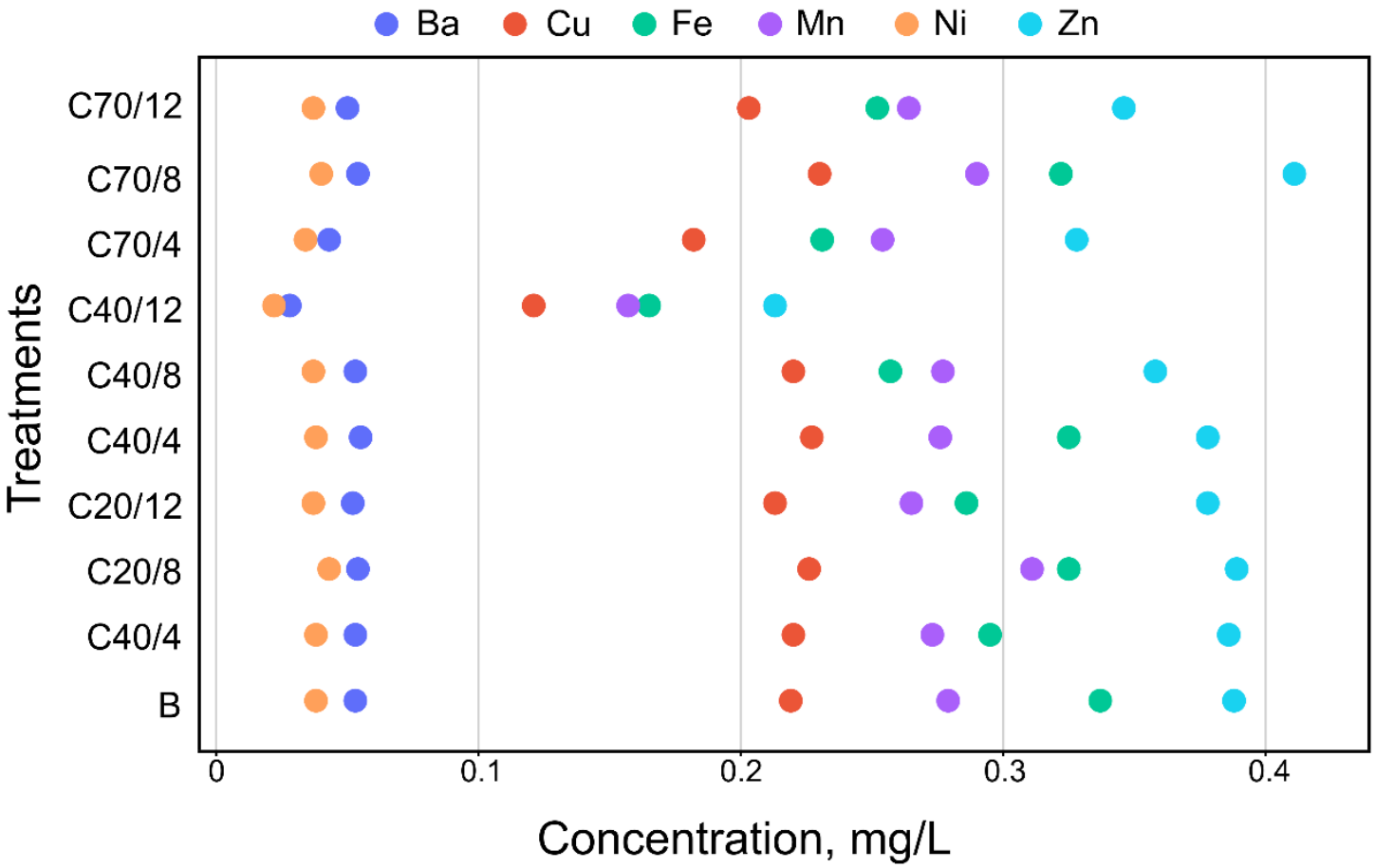

Figure 7

Micromineral content (Fe, Zn, Mn and Cu) of cacauí seed powder as affected by ultrasound pretreatment at amplitudes of 20, 40 and 70% for 12 min.